One-dimensional dynamics of lattice thermal transport

J. Phys.: Condens. Matter **9** (1997) 10867–10879. Printed in the UK PII: S0953-8984(97)82801-9

One-dimensional dynamics of lattice thermal transport

W Frizzera†‖, G Viliani†, M Montagna†, A Monteil‡ and J A Capobianco§

† Istituto Nazionale per la Fisica della Materia and Dipartimento di Fisica Università di Trento, I-38050 Povo, Trento, Italy

‡ Laboratoire POMA—E.P.CNRS 0130, Université d'Angers, 2 Boulevard Lavoisier, 49045 Angers Cédex, France

§ Department of Chemistry and Biochemistry, Concordia University, 1455 de Maisonneuve Boulevard West, Montreal, H3G 1M8, Canada

Received 21 March 1997, in final form 28 July 1997

Abstract. Non-equilibrium molecular dynamics is used to investigate the energy transport in both disordered and anharmonic linear chains under thermal stress by analysing the contribution to thermal flow of the vibrational normal modes. A thermal balance of the normal-mode energy is built up by considering the anharmonic interaction and the coupling with the reservoirs. The non-equilibrium normal-mode dynamics is studied and it is shown that, for both harmonic and anharmonic systems, the steady-state lattice thermal conductivity is described by a set of stationary normal modes with broadened and overlapping Fourier spectra. The origin of the thermal gradient is discussed. Because of the small number of atoms the bulk conductivity cannot be established.

1. Introduction

It is well known that in dielectric solids the heat carriers are the vibrational excitations which are not exactly particle-like, as in classical gases or liquids. Whereas the Boltzmann theory has been successfully applied by Peierls [1] (in order to explain the lattice thermal conductivity in crystalline and isotopically disordered solids [2, 3]), this approach becomes less tractable when the disorder cannot be considered as a simple perturbation, as for example is the case for glasses. In fact, although there is general agreement on the temperature dependence of the conductivity of amorphous solids up to 10 K, this is no longer the case at higher temperatures where a phonon-like scattering description is probably inappropriate.

An alternative approach to the Peierls–Boltzmann theory was proposed by Lebowitz and co-workers who studied the non-equilibrium stationary state by means of Gibbs-type ensembles [4]. In this approach the stationary state is maintained by stochastic impulsive interactions between the system particles and the particles of two or more heat reservoirs at different temperatures. This analytical method was successfully applied to study the classical thermal conductivity of the fixed ends of harmonic ordered linear chains [5], predicting zero temperature gradient (except at edges, where a paradoxical exponential behaviour was found) leading to an infinite thermal conductivity. Nevertheless, the limitations of the analytical approach become apparent when the anharmonic interaction is present. Visscher and co-workers [6] (see also reference [7]) performed a numerical simulation based on this theory. They studied the thermal flow in mass-disordered linear chains and found that when

‖ E-mail: frizzera@science.unitn.it.

0953-8984/97/4910867+13$19.50

the disorder is sufficiently strong, anharmonicity enhances thermal conductivity, contrary to what is observed for crystalline solids. This effect is attributed to the phonon-assisted hopping of the localized normal-mode energy, and whether or not it is responsible for the increase of the thermal conductivity above 10 K for amorphous solids still remains a point of debate [8–15]. Matsuda and Ishii [16] performed a theoretical investigation of the normal modes in a one-dimensional isotopically disordered chain. They found an exact expression in closed form for the thermal conductivity in the isotopically disordered harmonic chain. Non-equilibrium molecular dynamics has subsequently been applied for both one- and two-dimensional systems to test the independence of the thermal conductivity coefficient of the number of particles, the ergodic behaviour etc [17].

The purpose of this paper is to study the problem of thermal conductivity by means of a harmonic analysis of the energy, through the investigation of the normal-mode dynamics and the contribution of the modes to the energy transport. Section 2 gives an outline of the method of simulation used. In section 3.1 we discuss the results of the numerical analysis of thermal flow in harmonic chains. In section 3.2 we consider the effects of the anharmonicity on disordered linear chains. In section 3.3 we study the effects of the thermal reservoirs on the normal-mode dynamics and section 4 is devoted to the conclusions.

2. Outline of the method

In this section we describe the model and give a brief outline of the non-equilibrium molecular-dynamics method which has been clearly explained in reference [6].

We consider a fixed-end linear chain of N masses m_i $(i = 1, \ldots, N)$ which can be described by the Hamiltonian

$$H = \sum_{i=1}^{N} \frac{1}{2} m_i v_i^2 + \frac{\gamma}{2} \sum_{i=0}^{N} (u_{i+1} - u_i)^2 + \frac{\mu}{3} \sum_{i=0}^{N} |u_{i+1} - u_i|^3 \tag{1}$$

where u_i is the scalar displacement of the mass m_i from its equilibrium position ($u_0 = u_{N+1} = 0$), and γ and μ are the harmonic and anharmonic potential coefficients, respectively, which can be derived via an expansion of the Lennard-Jones potential [6]. In order to introduce anharmonicity while avoiding the melting of the system, we choose an even cubic anharmonic potential. The stationary state is maintained by replacing the velocity of the end atoms according to the Maxwell distribution

$$n_\alpha(w) = \left(\frac{M_\alpha}{2\pi k_B T_\alpha^{(R)}} \right)^{1/2} \exp\left(-\frac{M_\alpha w^2}{2k_B T_\alpha^{(R)}} \right) \tag{2}$$

where $T_\alpha^{(R)}$ $(\alpha = 1, N)$ are the temperatures of the thermal reservoirs and M_α is the mass of the atoms of the αth reservoir. Successive replacement velocities are chosen each time at random from the entire range of the distribution. The masses M_α have been taken to be equal to the end masses m_α. Because the distribution equation (2) is zero-centred, the sign of the gas mass velocities w is randomized, and thus the end particles experience collision with a vanishing average momentum. The time intervals between successive changes are chosen each time at random in the interval $[\lambda_a^{-1}, \lambda_b^{-1}]$, corresponding to an average coupling $\bar{\lambda}^{-1} = (\lambda_a^{-1} + \lambda_b^{-1})/2$. This procedure is useful in studying the limit of small coupling coefficients ($\lambda \to 0$), for avoiding finite-size effects. Initial positions and velocities are chosen randomly. The dynamical values and parameters are expressed in the units specified in reference [6] where the Boltzmann constant k_B and the harmonic coefficient γ are set to unity.

3. Results and discussion

3.1. Mode flow analysis

In this section we investigate the contribution of the vibrational normal modes to the thermal flow in the non-equilibrium steady state. The method presented in this paper is applied to the linear chain; however, it may also be applied to systems of higher dimensionality taking into account that the time necessary for the calculation is proportional to N^2.

The normal real coordinates are defined by

$$Q_k(t) = \sum_{i=1}^{N} \sqrt{m_i}\eta_{ik}u_i(t) \tag{3}$$

$$P_k(t) = \sum_{i=1}^{N} \sqrt{m_i}\eta_{ik}v_i(t) \tag{4}$$

where the η_{ik} are the eigenvectors, with eigenvalues ω_k^2, of the dynamical matrix of the harmonic Hamiltonian, with $\mu = 0$ in equation (1). For the fixed-end chain these are given by

$$\eta_{ik} = \sqrt{\frac{2}{N+1}}\sin(q_k i a) \qquad \omega_k = 2\sqrt{\frac{\gamma}{m}}\sin\left(\frac{q_k a}{2}\right) \tag{5}$$

with

$$q_k = \frac{\pi}{(N+1)a}k \qquad k = 1, \ldots, N. \tag{6}$$

When disorder is present they are obtained by numerical diagonalization. Due to the orthonormality of the eigenvectors the linear transformation equations (3) and (4) can be inverted and when substituted in equation (1) they diagonalize the harmonic contribution:

$$H = \frac{1}{2}\sum_{k=1}^{N}(P_k^2 + \omega_k^2 Q_k^2) + \frac{\mu}{3}\sum_{i=0}^{N}|u_{i+1} - u_i|^3 \tag{7}$$

where $H_k = \frac{1}{2}(P_k^2 + \omega_k^2 Q_k^2)$ is the energy of the mode k if the system is harmonic. In ordered chains we put $m_i = 1$ ($i = 1, \ldots, N$), and disorder is randomly introduced by isotopic impurities of mass 3. Thus, since the harmonic force γ is set to be unity, the frequencies will always be less than $\omega_s = 2$.

We now consider the harmonic chain ($\mu = 0$) in thermal contact with the two reservoirs at different temperatures $T_1^{(R)}$ and $T_N^{(R)}$ ($T_N^{(R)} > T_1^{(R)}$) characterized by the Maxwell distribution equation (2). Between the collisions, when the system is isolated and in the absence of anharmonicity, the normal coordinates follow the Heisenberg equations of motion ($P_k = \dot{Q}_k$):

$$\ddot{Q}_k(t) + \omega_k^2 Q_k(t) = 0 \tag{8}$$

$$\ddot{P}_k(t) + \omega_k^2 P_k(t) = 0. \tag{9}$$

We note that if the eigenpairs η_{ik} and ω_k are known, the temporal evolution can be calculated for given initial conditions using three steps: the linear transformations (3) and (4), the equations of motion (8) and (9), and finally the inverse transformations:

$$u_i(t) = \frac{1}{\sqrt{m_i}}\sum_{k=1}^{N}\eta_{ik}Q_k(t) \tag{10}$$

$$v_i(t) = \frac{1}{\sqrt{m_i}}\sum_{k=1}^{N}\eta_{ik}P_k(t). \tag{11}$$

Thus the time interval between collisions when the system is isolated can be covered with just one dynamical step, leading to a computing time $\propto N^2$. In harmonic systems this method represents an alternative way of integrating the equations of motion without using the step-by-step finite-difference methods (see references [18, 19]). However, it is only applicable if the eigenvectors and the eigenvalues of the dynamical matrix are known. Consequently it requires a diagonalization and it is only applicable to systems having a small number of particles. The advantage of this method is that it only introduces round-off errors and it is very effective, especially if one wants to increase the time interval between the collisions ($\lambda \to 0$). In the anharmonic chain we use a fourth-order Runge–Kutta algorithm with a time step $\mathrm{d}t = 0.01$ in order to solve the equations of motion step by step (higher frequencies are typically 2).

Because of the linear transformations given by equations (3) and (4) it is possible using molecular dynamics to compute at any time the mode energy H_k given in equation (7). Specifically, at each collision the mode energy H_k changes because of the abrupt variations in boundary mass velocity. This can easily be seen from equations (4) and (7). The collisions maintain the particle positions unaltered and thus also the potential contribution $\omega_k^2 Q_k^2/2$ to the mode energy H_k. Conversely the kinetic contribution $P_k^2/2$ changes and thus the integrated flows for the mode k at the end (α) of the chain are given by

$$\Phi_k^{(\alpha)}(t) = \sum_{\text{coll.}(\alpha)} \left(\frac{1}{2} P_{(\alpha)k}'^2 - \frac{1}{2} P_{(\alpha)k}^2 \right) \tag{12}$$

where the sum is over the collisions at the end $\alpha = 1$ or at $\alpha = N$ up to time t, and $P'_{(\alpha)k}$ and $P_{(\alpha)k}$ are given by equation (4), respectively after and before the collision at the end (α). The integrated mode flows $\Phi_k^{(\alpha)}(t)$ show a good linear time dependence when the steady state is achieved, and the mode flows $J_k^{(\alpha)}$ are the average slopes of the $\Phi_k^{(\alpha)}(t)$:

$$J_k^{(\alpha)} = \left\langle \frac{\mathrm{d}}{\mathrm{d}t} \Phi_k^{(\alpha)}(t) \right\rangle_t \tag{13}$$

where $\langle \cdots \rangle_t$ indicates the time average. Using the orthonormality of the eigenvectors it is not difficult to show that

$$\sum_{k=1}^{N} \Phi_k^{(\alpha)}(t) = \sum_{\text{coll.}(\alpha)} \left(\frac{1}{2} m_\alpha v_\alpha'^2 - \frac{1}{2} m_\alpha v_\alpha^2 \right) = \Phi^{(\alpha)}(t) \tag{14}$$

where the $\Phi^{(\alpha)}(t)$ are the integrated flows.

Let us consider an ordered chain of $N = 50$ masses with a coupling constant between $\lambda_a = 0.033$, corresponding to one collision every $\Delta t = 30$, and $\lambda_b = 0.017$, corresponding to one collision every $\Delta t = 60$ (that is, λ^{-1} is in the interval $[30, 60]$ and $\bar{\lambda}^{-1} = 45$), representing a small coupling coefficient (if the lattice constant is set to unity, the velocity of sound is $v_s = 1$ and the chain length is $L = 50$). After allowing an initial period to establish the steady state the integrated mode flows were calculated using equation (12) for approximately 2.2×10^7 collisions at both ends, corresponding to a running time $T \approx 10^9$ and to an integrated energy flow $|\Phi^{(\alpha)}(T)| \approx 3 \times 10^8$. The bath temperatures were $T_1^{(R)} = 25$ and $T_N^{(R)} = 75$.

Matsuda and Ishii [16] (see also references [20–22]) determined theoretically an expression for the mode flows J_k in the harmonic, fixed-end linear chain in the limit $\lambda \to 0$:

$$J(\lambda, N) = \lambda (T_N^{(R)} - T_1^{(R)}) \sum_{k=1}^{N} \frac{\eta_{1k}^2 \eta_{Nk}^2}{\eta_{1k}^2 + \eta_{Nk}^2} \tag{15}$$

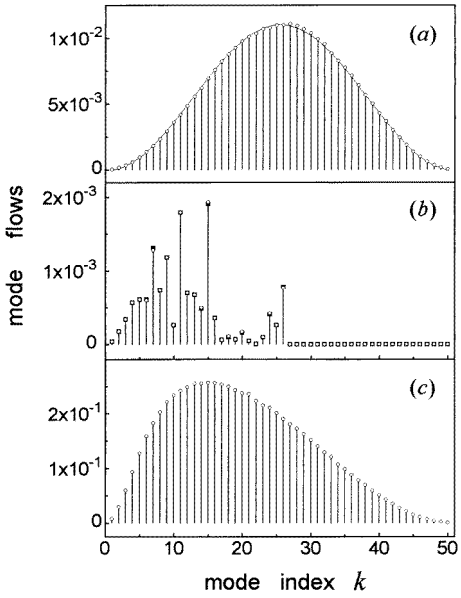

Figure 1. Mode flows $J_k^{(N)}$ in the harmonic chain of $N = 50$ masses and with reservoir temperatures $T_1^{(R)} = 25$ and $T_N^{(R)} = 75$. (*a*) A chain without mass disorder ($m_i = \gamma = 1$) and with λ^{-1} in the interval $[30, 60]$ and $\bar{\lambda}^{-1} = 45$. The bars ending with open circles indicate the results of the simulation. The solid line interpolating between the circles is given by equation (15). (*b*) A 50% randomly disordered chain of masses 1 and 3; λ^{-1} is in the interval $[30, 60]$ and $\bar{\lambda}^{-1} = 45$. The bars ending with open circles indicate the results of the simulation. The filled squares interpolating between the circles are given by equation (15). (*c*) An ordered chain with λ^{-1} in the interval $[0.8, 1]$ and $\bar{\lambda}^{-1} = 0.9$.

where η_{1k} and η_{Nk} are the amplitudes (the end masses are set to unity) of the mode k at the chain ends. The theoretical prediction, equation (15), and the numerical calculation of $J_k^{(N)}$ given by equation (13) are shown for the ordered harmonic chain in figure 1(*a*).

The result is that, in the harmonic systems, each mode gives to the cold reservoir the same energy as is received from the hot one; that is, $J_k^{(1)} = -J_k^{(N)}$. Therefore, in finite-size systems the reservoirs do not couple the modes when the system is purely harmonic although they do affect the normal-mode dynamics which will be discussed in section 3.3. This agrees with the fact that the harmonic systems are described by a set of non-interacting normal modes. Moreover, with fixed boundary conditions low- and high-frequency modes have small amplitudes at the end sites, and hence they do not contribute appreciably to the transport. The theoretical prediction, equation (15), and the numerical calculation of $J_k^{(N)}$ given by equation (13) are shown for a 50% randomly disordered chain in figure 1(*b*). Thus equation (15) fits the mode flows very well, demonstrating the validity of both the numerical and theoretical calculations, the latter based on the IF assumption [16]. In comparison to the analytical approach (suitable only for 1D and in the limit $\lambda \to 0$), the numerical method has an intrinsic advantage because it is possible to increase the coupling constant λ and, in principle, it is applicable to both two- and three-dimensional systems as well as anharmonic systems. For example, in figure 1(*c*) the mode flows $J_k^{(N)}$ are shown for the harmonic linear chain with larger coupling constants: λ^{-1} in the interval $[0.8, 1]$ and $\bar{\lambda}^{-1} = 0.9$. In the limit $\lambda \to 0$, the flows depend only on the amplitudes of the modes at the boundaries of the chain, but when λ increases, the low-frequency modes are relatively effective in carrying

the energy. This can be intuitively interpreted by means of wave-packet group velocities. Since the latter is lower in high-frequency modes, more time is needed to carry the energy out, such that it is returned to the baths.

3.2. The anharmonic flows

Using the variables P_k and Q_k defined in equations (3) and (4), an energy balance is established for the harmonic mode energy H_k, which is time dependent due to the interactions with the reservoirs and anharmonicity.

Let us consider the same disordered chain as in figure 1(*b*) but with added anharmonicity ($\mu = 0.35$ in equation (1)). The mode flows (not reported here) have been computed as for the harmonic chain, with an inverse coupling coefficient λ^{-1} in the interval $[1.3, 1.5]$ ($\bar{\lambda}^{-1} = 1.4$) and approximately 4×10^6 collisions at both ends. The bath temperatures were $T_1^{(R)} = 25$ and $T_N^{(R)} = 75$. In calculating $\Phi_k^{(\alpha)}(t)$ using equation (12) it is unnecessary to assume that the system is harmonic, and the relationship given by equation (14) is still valid. We observed that in general, due to the anharmonic interaction, some modes receive energy from the hot reservoir but they do not return the same quantity to the cold reservoir, and vice versa. That is, $J_k^{(1)} \neq -J_k^{(N)}$, which is not the case for the harmonic systems. It is possible to account for the difference by calculating the anharmonic integrated flows $\Phi_k^{(A)}(t)$ defined by

$$\Phi_k^{(A)}(t) = \sum_{\text{coll.}} (H_k' - H_k) \tag{16}$$

where H_k is the energy of the mode k just after a collision and H_k' is the mode energy just before the next one. The flows $\Phi_k^{(A)}(t)$ differ from the flows $\Phi_k^{(\alpha)}(t)$ because the latter are computed before and after the same collision. The sum in equation (16) is for collisions at both ends up to time t. From simulation it is found that, like the $\Phi_k^{(\alpha)}(t)$, the $\Phi_k^{(A)}(t)$ are linearly increasing functions. This implies that, because of the anharmonicity, a stationary energy flow between the modes takes place. Moreover, at each simulation step the equality

$$H(t) = H(0) + \Phi^{(1)}(t) + \Phi^{(N)}(t) \tag{17}$$

must be satisfied. In equation (17), $H(t)$ and $H(0)$ are the total energies (harmonic + anharmonic) at time t and immediately after the thermalization at $t = 0$, respectively, and the $\Phi^{(\alpha)}(t)$ are the integrated flows at time t. Equation (17) is simply the energy balance of the system. From equation (14), the integrated flows $\Phi^{(\alpha)}(t)$ can be written as sums of integrated flows relative to the modes, and the balance equation (17) can be shown to be

$$\sum_{k=1}^{N} H_k(t) + H^{(A)}(t) = \sum_{k=1}^{N} H_k(0) + H^{(A)}(0) + \sum_{k=1}^{N} \Phi_k^{(1)}(t) + \sum_{k=1}^{N} \Phi_k^{(N)}(t) \tag{18}$$

where the harmonic and the anharmonic contributions to $H(t)$ and $H(0)$ have been explicitly written out and $H^{(A)}$ is given by the second term in the right-hand side of equation (7). On the other hand, employing equation (16), a mode balance can be written as follows:

$$H_k(t) = H_k(0) + \Phi_k^{(A)}(t) + \Phi_k^{(1)}(t) + \Phi_k^{(N)}(t) \tag{19}$$

where $H_k(0)$ is the energy of the mode k at the time $t = 0$. The balance equation (19) includes changes in mode energy because of the collisions and the anharmonic interactions. This balance is also representative for harmonic systems for which $\Phi_k^{(A)}(t) = 0$, since the normal modes do not interact, and the mode energy is conserved between the collisions when the system is isolated. Because $\Phi_k^{(A)}(t)$, $\Phi_k^{(1)}(t)$ and $\Phi_k^{(N)}(t)$ are linearly increasing

time functions and the mode energy $H_k(t)$ remains limited, it is seen from equation (19) that $[(\Phi_k^{(A)}(t) + \Phi_k^{(1)}(t) + \Phi_k^{(N)}(t))]/t$ is limited above by a quantity that goes to zero as $1/t$ in the limit $t \to \infty$. Thus by averaging in equation (19), the following balance for the mode flows is obtained:

$$J_k^{(A)} + J_k^{(1)} + J_k^{(N)} = 0 \tag{20}$$

where

$$J_k^{(A)} = \left\langle \frac{\mathrm{d}}{\mathrm{d}t} \Phi_k^{(A)}(t) \right\rangle_t . \tag{21}$$

Moreover, by substituting equation (19) into equation (18) we obtain

$$\sum_{k=1}^{N} \Phi_k^{(A)}(t) + H^{(A)}(t) = H^{(A)}(0) \tag{22}$$

and since the anharmonic energy remains limited, we have $[(\sum_k \Phi_k^{(A)}(t))]/t \to 0$ like $1/t$ in the limit $t \to \infty$. Taking an average derivative of equation (22), we have

$$\sum_{k=1}^{N} J_k^{(A)} = 0. \tag{23}$$

In conclusion, since in the steady state the mean energies in each mode and the anharmonic energy do not vary with time, and since the anharmonic energy can be exchanged only with the modes and not with the heat baths, equations (20) and (23) must follow.

3.3. Steady-state normal-modes dynamics

In sections 3.1 and 3.2 we have considered the thermal flow by analysing how each normal mode contributes to it. In this section we investigate the following question: how does the dynamics of the normal coordinates (Q_k, P_k) explain the thermal gradient and the stationary flow?

If the system is harmonic and isolated, the solutions of the Heisenberg equations of motion for the normal coordinates are given by equations (8) and (9) which represent harmonic oscillators for both $P_k(t)$ and $Q_k(t)$ at frequencies ω_k. However, when the system interacts with an external system such as a heat reservoir, the harmonic equations of motion are no longer satisfied. It is not possible to keep both the flow and gradient stationary simply by choosing some particular initial condition (Q_k^0, P_k^0) in equations (8) and (9). The local temperature T_i can be written using the transformation equation (11) in terms of normal momenta $P_k(t)$:

$$T_i \equiv 2\left\langle \frac{1}{2} m_i v_i^2(t) \right\rangle_t = \sum_{k,k'=1}^{N} \eta_{ik}\eta_{ik'} \langle P_k(t) P_{k'}(t) \rangle_t = T_i^{(1)} + T_i^{(2)} \tag{24}$$

where $T_i^{(1)}$ and $T_i^{(2)}$ are respectively the diagonal and off-diagonal contributions to T_i:

$$T_i^{(1)} = \sum_{k=1}^{N} \eta_{ik}\eta_{ik} \langle P_k(t) P_k(t) \rangle_t \tag{25}$$

and

$$T_i^{(2)} = \sum_{k \neq k'}^{N} \eta_{ik}\eta_{ik'} \langle P_k(t) P_{k'}(t) \rangle_t . \tag{26}$$

Moreover the instantaneous flow may be calculated by taking the time average of the expression [1, 23, 24]

$$J(t) = \frac{1}{2N}\sum_{i=0}^{N}\gamma[u_{i+1}(t) - u_i(t)][v_{i+1}(t) + v_i(t)] \tag{27}$$

where N is the dimensionless volume of the lattice (the harmonic force constant γ is set to be unity). Equation (27) is essentially the quadratic part of the harmonic flow operator as given by Hardy [25]. Thus, the average flow $\langle J(t)\rangle_t \equiv J$ can also be written in terms of the (Q_k, P_k) variables by means of the transformations of equations (10) and (11):

$$J = \frac{1}{2N}\sum_{k,k'=1}^{N}\left[\sum_{i=0}^{N}\left(\frac{\eta_{i+1k}}{\sqrt{m_{i+1}}} - \frac{\eta_{ik}}{\sqrt{m_i}}\right)\left(\frac{\eta_{i+1k'}}{\sqrt{m_{i+1}}} + \frac{\eta_{ik'}}{\sqrt{m_i}}\right)\right]\langle Q_k(t)P_{k'}(t)\rangle_t. \tag{28}$$

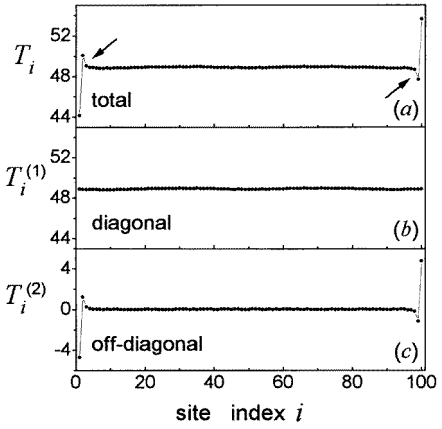

Figure 2. (*a*) The local temperature T_i in the harmonic chain without mass disorder. Here, $N = 100$, $T_1^{(R)} = 25$ and $T_N^{(R)} = 75$, $m_i = \gamma = 1$, λ^{-1} is in [1.5, 2], $\bar{\lambda}^{-1} = 1.75$. (*b*) and (*c*) show the diagonal and off-diagonal contributions to T_i, respectively (see equations (25) and (26)). The arrows in (*a*) indicate the exponential decays observed away from the boundaries.

It appears from equations (24) and (28) that the averages $\langle P_k(t)P_{k'}(t)\rangle_t$ and $\langle Q_k(t)P_{k'}(t)\rangle_t$ are quantities which can be investigated in order to understand the normal-mode dynamics in the stationary state of the thermal conductivity. This can be done numerically by calculating the time averages $\langle P_k(t)P_{k'}(t)\rangle_t$ and $\langle Q_k(t)P_{k'}(t)\rangle_t$ by sampling $P_k(t)$ and $Q_k(t)$, using equations (3) and (4), in regular step intervals. Each signal $P_k(t)$ can be approximated by a truncated Fourier series:

$$P_k(t) = \sum_{j=0}^{N_s-1} c_j(k)\exp\left(\frac{\mathrm{i}\,2\pi jt}{P}\right) \tag{29}$$

where N_s is the number of samples, P is the time interval chosen arbitrarily for the Fourier analysis (P was the same for each k) and $c_j(k)$ is the jth complex Fourier component of $P_k(t)$. If P is sufficiently large, the averages in equation (24) are the overlap integrals of the $P_k(t)$ and $P_{k'}(t)$ Fourier spectra:

$$\langle P_k(t)P_{k'}(t)\rangle_t = \sum_{j=0}^{N_s-1} c_j(k)c_j^*(k'). \tag{30}$$

As shown below, the time averages in equations (24) and (28) have a well defined structure and do not vanish even if $k \neq k'$. From equation (30) it can be seen that the normal modes k and k' cannot have Fourier components $c_j(k)$ and $c_j^*(k')$ which simultaneously vanish for each index j; that is, the normal modes k and k' must have some common frequency of vibration. Thus the reservoirs introduce new frequencies in the oscillation spectrum of each mode, causing degeneracy of the states.

We consider first the ordered chain ($m_i = 1$, $i = 1, \ldots, N$, $N = 100$) with an inverse coupling constant λ^{-1} in the interval [1.5, 2] ($\bar{\lambda}^{-1} = 1.75$) and bath temperatures $T_1^{(R)} = 25$ and $T_N^{(R)} = 75$. The averages in equation (24) have been calculated for approximately 1.7×10^7 samples with a sampling interval $\Delta t = 1.5$, for a running time $T \approx 2.6 \times 10^7$, and what amounts to about 1.5×10^7 collisions at both ends. In figure 2(a) the local temperature T_i for the harmonic ordered chain is shown. The local temperature is constant except at the boundaries, where drops of local temperature above and below the mean temperature, for the second mass $i = 2$ and penultimate mass $i = N - 1$, respectively, appear. The temperature decreases exponentially along the chain as indicated by the arrows. This paradoxical result was first observed by Lebowitz and co-workers [5] theoretically investigating the stationary state in the harmonic ordered chain. In figure 2(b) the diagonal contribution $T_i^{(1)}$ is shown and it shows a constant profile. This means that the normal modes have a frequency-independent mean energy $\langle P_k(t)^2 \rangle_t$, which can be deduced from equations (25) and by taking into account the orthonormality of the eigenvectors. Figure 2(c) shows the off-diagonal contribution $T_i^{(2)}$ which is responsible for deviations from a uniform temperature profile.

The averages in equation (24) have a well defined structure. Let δ in $\langle P_k(t) P_{k+\delta}(t) \rangle_t$ be the index of the δth codiagonal ($\delta = 0$ is the main diagonal) of the matrix $(\langle P_k(t) P_{k'}(t) \rangle_t)$. Thus $\delta = 0, \ldots, N - 1$ for the upper codiagonals and $k = 1, \ldots, N - \delta$ is the index of the corresponding elements. Only odd-delta terms ($\delta = 1, 3, \ldots, N - 1$) contribute to the apparent thermal gradient while the even terms ($\delta = 2, 4, \ldots, N - 2$) are vanishing. Figure 3(a) shows the averages $\langle P_k(t) P_{k+\delta}(t) \rangle_t$ with $\delta = 1, 3, \ldots, N - 1$. Moreover, the dips at sites $i = 2$ and $i = N - 1$ are due to the hump indicated by the arrow in figure 3(a). In fact let us consider the site $i = 1$. In figure 3(b) the products $\eta_{1k} \eta_{1k+\delta}$ with odd δ are shown. To obtain one half of the off-diagonal local temperature of site $i = 1$, we must multiply and sum term by term all the corresponding points of figure 3(a) and figure 3(b), as required by equation (26). This summation is negative as shown in figure 2(c) because of the greater contribution to $\sum \eta\eta \langle P\,P \rangle_t$ which comes from terms where $\eta\eta$ is positive and $\langle P\,P \rangle_t$ is negative. Figure 3(c) is the same as figure 3(b) except at the site $i = 2$. In this case the products $\eta_{2k} \eta_{2k+\delta}$ vanish for $k \approx 50$, and the terms $\eta\eta \langle P\,P \rangle_t$ are negligible in this region. Conversely they become important for small k where both $\langle P\,P \rangle_t$ and $\eta\eta$ are positive and the off-diagonal contribution to T_2 is positive as shown in figure 2(c). On increasing the site position the off-diagonal contribution vanishes since the oscillation frequency of the products $\eta\eta$ increases and thus T_i is only determined by the diagonal constant temperature. On the right-hand side, the behaviour is specular because the products $\eta\eta$ have opposite signs.

We note that the coherent transport, which leads to a vanishing gradient far from the boundaries, is equivalent to a lack of correlation between the products $\eta\eta$ and $\langle P\,P \rangle_t$ [26]. Moreover, it appears that the dips in T_2 and T_{N-1} arise because, in one-dimensional fixed-end systems, the modes of relatively low frequency (the small-k region in figure 3(a)) tend to contribute to building up a thermal gradient in a way opposite to that imposed by the reservoirs. No explanation is given for this paradoxical behaviour.

We now consider the thermal flow. When the system is isolated, $Q_k(t)$ and $P_k(t)$

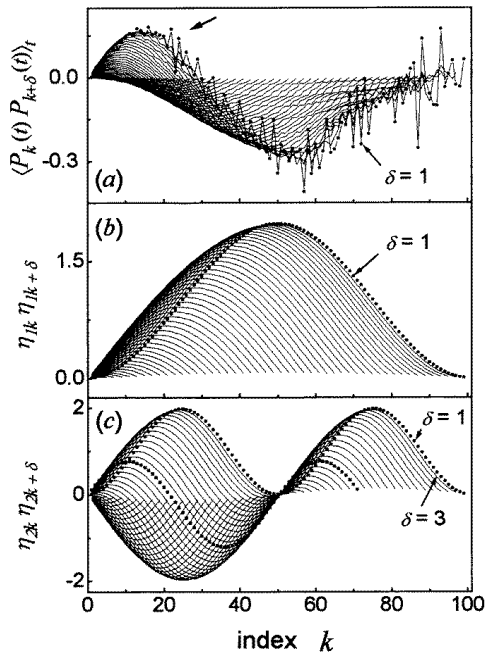

Figure 3. Plots for the chain of figure 2. In (*a*) the averages $\langle P_k(t)P_{k+\delta}(t)\rangle_t$ are shown. The arrow points to the hump which is responsible for the dips in T_2 and T_{N-1} shown in figure 2(*a*) (see the text). In (*b*) and (*c*) the products $\eta_{1k}\eta_{1k+\delta}$ ($\times 10^2$) and $\eta_{2k}\eta_{2k+\delta}$ ($\times 10^2$), respectively, are shown. The curves with full circles are relative to $\delta = 1$ and the successive curves correspond to $\delta = 3, 5, \ldots, N-1$ with $k = 1, \ldots, N-\delta$.

satisfy equations (8) and (9) and consequently the averages $\langle Q_k(t)P_{k'}(t)\rangle_t$ vanish no matter how phase relations (Q_k^0, P_k^0) are chosen. Thus, because the averages $\langle Q_k(t)P_{k'}(t)\rangle_t$ enter directly into the expression for the thermal flow, equation (28), a steady thermal flow cannot be explained by the equilibrium equation of motion for the normal coordinates. This is a peculiarity of fixed and real free boundary conditions where the normal modes are stationary waves. However, it is not the case when we impose periodic boundary conditions due to the fact that the eigenstates can also be travelling waves (phonons) with wave vector q or $-q$, and it is possible to put the system into a state $\langle Q_q(t)P_{-q}(t)\rangle_t = \langle Q_{-q}(t)P_q(t)\rangle_t^* \neq 0$, and equation (28) leads to the diagonality of the heat flow operator [1, 25]:

$$J = \frac{1}{N}\sum_q H_q \frac{\partial\omega(q)}{\partial q} \tag{31}$$

where H_q is the energy of the mode with wave vector q and $\partial\omega(q)/\partial q$ is its group velocity [27]. The problem of finding an expression for the thermal flow is simplified by choosing periodic boundary conditions or, more generally, a travelling-wave picture as noted by Peierls [28]. Nevertheless it is not possible to fit the mode flows shown in figure 1(*a*) by using equation (31). This behaviour originates from the finite width of the frequencies when the harmonic system is not at equilibrium, and the averages $\langle Q_k(t)P_{k'}(t)\rangle_t$ entering in equation (28) do not vanish because the modes have some degree of degeneracy. The link with the microscopical analysis of mode flows (see section 3.1) can be obtained by

numerically summing in equation (28) over labels i and for example k' after the calculation of $\langle Q_k(t)P_{k'}(t)\rangle_t$. Thus the flow can formally be considered as a summation of mode flows, $J = \sum_k J_k$. These differ by less than 3–4% from the mode flows calculated with the method described in section 3.1. It is worth noting that the properties of the averages $\langle P_k(t)P_{k'}(t)\rangle_t$ and $\langle Q_k(t)P_{k'}(t)\rangle_t$ are essentially those of the non-equilibrium correlation functions $\langle v_i(t)v_j(t)\rangle_t$ and $\langle u_i(t)v_j(t)\rangle_t$, which are related by the definitions of normal coordinates, equations (3) and (4), and the inverse transformations given by equations (10) and (11).

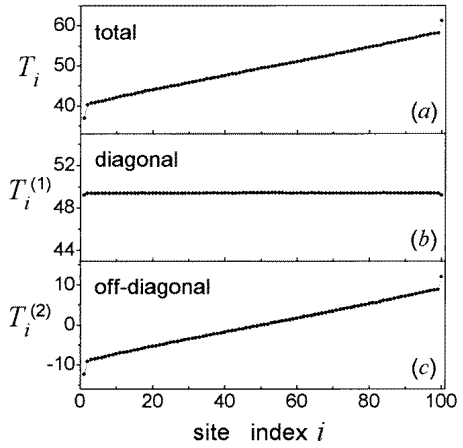

Figure 4. (a) The local temperature T_i in the anharmonic chain without mass disorder. (b) and (c) show the diagonal and off-diagonal contributions to T_i, respectively (see equations (25) and (26)). $N = 100$, $m_i = \gamma = 1$, $\mu = 0.35$, $T_1^{(R)} = 25$, $T_N^{(R)} = 75$, λ^{-1} is in $[1.5, 2]$, $\bar{\lambda}^{-1} = 1.75$.

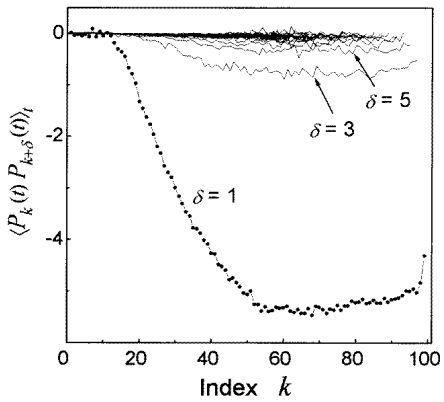

Figure 5. Plots of $\langle P_k(t)P_{k+\delta}(t)\rangle_t$ as in figure 3(a), but for the anharmonic ordered chain of figure 4.

The numerical method allows general applications not restricted to the one-dimensional harmonic ordered systems. We considered the anharmonic ordered chain with an anharmonicity coefficient μ of 0.35 in equation (1). The inverse coupling constant λ^{-1} is in the interval $[1.5, 2]$ ($\bar{\lambda}^{-1} = 1.75$) with numbers of collisions of about 3×10^6 and 5×10^6, averages taken with a sampling step $\Delta t = 1$ and bath temperatures of $T_1^{(R)} = 25$ and $T_N^{(R)} = 75$. Figures 4(a), 4(b), 4(c) show the local temperature T_i and the diagonal and off-diagonal contributions to T_i, respectively. As in the harmonic chain, the thermal gradient is completely determined by the off-diagonal contributions. The averages $\langle P_k(t)P_{k+\delta}(t)\rangle_t$, with $\delta = 1, 3, \ldots, N-1$, are shown in figure 5. Terms with even δ (except $\delta = 0$) are still negligible. The curves in figure 5 explain the thermal gradient of figure 4(a). In fact the averages $\langle P_k(t)P_{k+\delta}(t)\rangle_t$ are always negative, contrary to what happens in the harmonic chain as seen in figure 3(a). Moreover the most important terms are $\langle P_k(t)P_{k+1}(t)\rangle_t$. Secondly, the products $\eta_{ik}\eta_{ik+\delta}$ gradually change from completely positive values ($i = 1$) to completely negative ones ($i = N$) [29]. We conclude that there is a local temperature determined by the diagonal terms in equation (24) which are essentially the k-independent mode energies $\langle P_k^2\rangle_t$. Moreover in going from $i = 1$ to $i = N$ we must add to the diagonal terms the off-diagonal ones whose sign gradually changes. This leads to a non-vanishing smooth gradient as shown in figure 4(a).

4. Conclusions

In figure 5 we observe that there is no contribution to the off-diagonal temperature from the low-frequency products $\langle P\,P\rangle_t$. Thus, low-frequency modes do not contribute significantly to the forming of the gradient. For a given strength of coupling λ, the mode flows are found to be proportional to the thermal gradient, giving an effective coefficient of thermal conductivity. However, the flows are generally very sensitive to changes in λ—see, e.g., figures 1(a) and 1(c)—while the thermal gradient is much less sensitive. Consequently the effective thermal conductivity coefficient depends strongly on λ. Specifically, it increases with λ over a wide range.

When λ becomes large, the dips in T_2 and T_{N-1} shown in figure 2(a) diminish together with the hump indicated by the arrow in figure 3(a). At the same time, the curves of figure 3(a) become similar (with opposite sign) to those of figure 3(b). That is, if $i \neq 1$ or $i \neq N$, the δth codiagonal ($\langle P_k(t)\,P_{k+\delta}(t)\rangle_t$) becomes orthogonal to the δth vector ($\eta_{ik}\eta_{ik+\delta}$), for each δ. This has the effect that only the sites $i = 1$ and $i = N$ have a temperature different from the average. Actually, as seen in figure 2(a), this kind of orthogonality is partially satisfied independently of the strength of the coupling λ. In fact the hump indicated by the arrow in figure 3(a) is responsible only for the dips observed in T_2 and T_{N-1} and it does not in practice affect the local temperature which is uniform far from the boundaries. The different gradient observed in the anharmonic chain can be explained by different overlapping integrals (from the comparison of figure 5 and figure 3(a)). The orthogonality of the vectors $\langle P_k(t)\,P_{k+\delta}(t)\rangle_t$ and $\eta_{ik}\eta_{ik+\delta}$ is broken by the anharmonic coupling leading to a non-vanishing thermal gradient.

The method and results should be useful in the extension to two- and three-dimensional lattices.

Acknowledgments

We would like to thank M Wagner, G Ruocco, O Pilla and T Peres for useful discussions.

References

[1] Peierls R E 1929 *Ann. Phys. Lpz.* **3** 1055
[2] Klemens P G 1958 *Solid State Physics* vol 7 (New York: Academic) p 1
[3] Callaway J 1959 *Phys. Rev.* **113** 1046
[4] Lebowitz J L 1959 *Phys. Rev.* **114** 1192 and references therein
[5] Rieder Z, Lebowitz J L and Lieb E 1967 *J. Math. Phys.* **8** 1073
[6] Payton D N III, Rich M and Visscher W M 1967 *Phys. Rev.* **160** 706
[7] Jackson E A, Pasta J R and Waters J F 1968 *J. Comput. Phys.* **2** 207
[8] Jagannathan A, Orbach R and Entin-Wohlman O 1989 *Phys. Rev.* B **39** 13 465
[9] Allen P B and Feldman J L 1993 *Phys. Rev.* B **48** 12 581
Feldman J L, Kluge M D, Allen P B and Wooten F 1993 *Phys. Rev.* B **48** 12 589
[10] Michalsky J 1992 *Phys. Rev.* B **45** 7054
[11] Lee Y H, Biswas R, Soukoulis C M, Wang C Z, Chan C T and Ho K M 1991 *Phys. Rev.* B **43** 6573
Wang C Z, Chan C T and Ho K M 1990 *Phys. Rev.* B **42** 11 276
[12] Sheng P and Zhou M 1991 *Science* **253** 539
[13] Cahill D G, Watson S K and Pohl R O 1992 *Phys. Rev.* B **46** 6131
[14] Ladd A J C, Moran B and Hoover W G 1986 *Phys. Rev.* B **34** 5058
[15] Bickham S R and Feldman J L 1998 *Phil. Mag.* B at press
[16] Matsuda H and Ishii K 1970 *Prog. Theor. Phys. Suppl.* **45** 56
and see also
Ishii K 1973 *Prog. Theor. Phys. Suppl.* **53** 77

[17] For more recent applications of this method see, for example,
Poetzsch R H H and Böttger H 1994 *Phys. Rev.* B **50** 15 757 and references therein
[18] Vazquez-Marquez J, Wagner M, Montagna M, Pilla O and Viliani G 1991 *Physica* B **172** 355
[19] Wagner M, Lütze A, Viliani G, Frizzera W and Pilla O 1993 *Physica* B **190** 285
[20] O'Connor A J and Lebowitz J L 1974 *J. Math. Phys.* **15** 692
[21] Visscher W M 1971 *Prog. Theor. Phys.* **46** 729
[22] Visscher W M 1976 *Methods in Computational Physics* vol 15, ed G Gilat (New York: Academic) p 371
[23] Ranninger J 1965 *Phys. Rev.* **140** A2031
[24] Jackson E A 1978 *Rocky Mountain J. Math.* **8** 127
[25] Hardy R J 1963 *Phys. Rev.* **132** 168
[26] An analogous calculation based on solution of the covariance matrix has been carried out by Nakazawa for the linear harmonic ordered chain with free boundary conditions; see
Nakazawa H 1968 *Prog. Theor. Phys.* **39** 236
Nakazawa H 1970 *Prog. Theor. Phys. Suppl.* **45** 231
Nakazawa showed that in this case the temperature profile is constant along the chain except for the end masses. In any case, for both fixed and free ends a uniform local temperature appears away from the boundaries, which is usually interpreted as indicating an infinite thermal conductivity of these systems.
[27] If we label the modes in order of increasing frequency we have that, in the periodic chain, mode $k = 1$ is the translation, modes $k = 2$ and $k = 3$ build up the first travelling phonon etc. Thus the averages $\langle Q_q(t)P_{-q}(t)\rangle_t$ would correspond, in this notation, to $\langle Q_k(t)P_{k+1}(t)\rangle_t$ with even k. For a system with periodic boundary conditions it is not difficult to obtain the flow given by equation (31) by substituting the solution of equations (8) and (9) in equation (28) or more directly by substituting travelling waves for u_i and v_i in equation (27).
[28] Peierls R E 1955 *Quantum Theory of Solids* (Oxford: Oxford University Press) p 47
[29] The signs of the products $\eta_{ik}\eta_{ik+\delta}$ are to be considered relatively to those of the averages $\langle P_k(t)P_{k+\delta}(t)\rangle_t$ because the signs of the eigenvectors are arbitrary.